

Extended x-ray-absorption fine structure of liquid water

B. X. Yang and J. Kirz

Department of Physics, State University of New York at Stony Brook, Stony Brook, New York 11794

(Received 18 February 1987)

Extended x-ray-absorption fine structure (EXAFS) of liquid water above the oxygen *K* edge is reported for the first time. Major features of the EXAFS spectrum agree with the calculated spectrum based on the known O-O pair correlation function in water. Other features are tentatively identified as due to the effect of the hydrogen atoms on the photoelectrons.

The last decade has witnessed major developments in liquid physics. Computer-simulation studies of many model potentials¹ have been made with various algorithms, including a Feynman path-integral approach.² In experimental studies of liquid structure, x-ray diffraction achieved higher accuracy over a larger range of scattering variables.³ Neutron diffraction was successfully applied to water and aqueous solutions,⁴ and was used to determine the partial structure functions through isotope substitution.⁵ Electron diffraction from thin films of water has also been observed.⁶ The atomic pair correlation functions (APCF's) in heavy water were obtained from the combined analysis of x-ray, neutron, and electron diffraction data.⁶ While diffraction techniques have provided much valuable information, our understanding of the structure of water remains limited.

In this work, we report the first soft-x-ray extended x-ray-absorption fine-structure (EXAFS) experiment for the determination of liquid structure. EXAFS refers to the small-amplitude modulation of the absorption coefficient starting from a few tens of eV above an absorption edge. It is due to the modification of outgoing electron waves by neighboring atoms in photoionization. The phenomenon is used extensively as a structural tool in

studying short-range order.⁷

One of the advantages of the EXAFS technique is its elemental sensitivity. The atomic environment of each species can be separately studied by tuning the x-ray energy to its absorption edge. Another advantage is that under favorable conditions it yields information about three-body correlation functions. When an atom is located between the absorbing atom and the scattering atom, the scattering amplitude and phase shift can be modified significantly by the potential of the intervening atom (multiple scattering or focusing effect)⁸ and both are sensitive functions of the geometry. In water, this information may be useful for understanding the hydrogen bond, but may not be easily studied through other experimental techniques.

In the presence of EXAFS, the absorption coefficient is given by⁷ $\mu = \mu_B + \mu_0[1 + \chi(k)]$, where $k = [2m(E - E_0)]^{1/2}/\hbar$ is the photoelectron momentum, E_0 the ionization threshold, μ_0 the smooth atomiclike absorption coefficient for the core-level excited, and μ_B the background absorption coefficient. $\chi(k)$ is the EXAFS function which contains the structural information about the environment of the absorbing atom. For *K*-edge EXAFS of atomic species α , it can be written as⁷

$$\begin{aligned} \chi_\alpha(k) &= \frac{4\pi}{k} \sum_\beta \rho_\beta F_\beta \int_0^\infty g_{\alpha\beta}(r) e^{-2r/\lambda} \sin(2kr + \phi_{\alpha\beta}) dr \\ &= \frac{4\pi}{k} \sum_\beta \rho_\beta F_\beta \left[\frac{\lambda(\cos\phi_{\alpha\beta} - 2k\lambda \sin\phi_{\alpha\beta})}{2(1 + k^2\lambda^2)} + \int_0^\infty [g_{\alpha\beta}(r) - 1] e^{-2r/\lambda} \sin(2kr + \phi_{\alpha\beta}) dr \right], \end{aligned} \quad (1)$$

where ρ_β is the average density of atomic species β , $g_{\alpha\beta}$ the APCF between α and β , $F_\beta(k)$ the backscattering amplitude of β , $\phi_{\alpha\beta}(k)$ the phase shift due to the atomic potentials, and λ the mean free path of photoelectrons. In a real liquid, $g_{\alpha\beta} - 1$ approaches zero faster than $e^{-2r/\lambda}$, therefore the second form gives less truncation error.

A major experimental challenge of absorption spectroscopy in the soft-x-ray region is the preparation of homogeneous thin samples. With liquids, one must also provide a container with windows of sufficient transparency. Our experiment makes use of Si_3N_4 windows with a 1- μm -thick polymethylmethacrylate (PMMA) spacer to define the sample volume (Fig. 1). The experiment was per-

formed at the U15 beamline at the National Synchrotron Light Source, Brookhaven National Laboratory. The experimental procedure is as follows. We put a drop of distilled water on the front window, place the rear window over it, and carefully squeeze the excess water out of the cell through two channels in the spacer. We then add a few drops of water in the buffer chamber and pump the chamber down to the vapor pressure of water to remove the air. We take a few spectra with the chamber sealed and some water droplets remaining in it. After that, we pump the chamber continuously for about ten minutes to remove all the water in the buffer and in the cell (through the channels), and then take a spectrum of the empty cell.

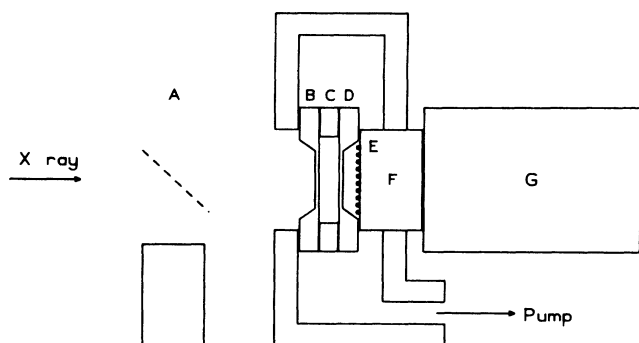


FIG. 1. Schematic diagram of the experimental setup. (A) I_0 monitor: P31 screen and PMT. The sample cell (B) front window: Si_3N_4 , $0.2 \text{ mm} \times 0.2 \text{ mm} \times 1500 \text{ \AA}$. (C) PMMA photoresist spacer with side channels. (D) Rear window: Si_3N_4 , $1 \text{ mm} \times 1 \text{ mm} \times 1500 \text{ \AA}$. I monitor (E) P31 phosphor, about 0.1 mm downstream of (D). (F) Light guide. (G) PMT. The space outside the cell forms a buffer chamber.

This procedure ensures that all spectra are taken under identical optical conditions. At the oxygen K edge the monochromator is accurate to about 1 eV . The x-ray flux is about 10^9 photons/sec of which $\leq 15\%$ is second-order radiation.⁹ A typical scan takes 20–50 min. The photomultiplier tubes (PMT's) operate in current mode. Their output, usually in the μA range, is digitized with current-to-frequency convertors and recorded by a PDP-11/23 computer through a CAMAC interface.

The raw data are shown in Fig. 2(a). In order to obtain the attenuation coefficient [Fig. 2(b)], the distortion due to the second-order radiation is corrected for with H_2O vapor absorption data, which were measured with an apparatus described elsewhere.¹⁰ Features due to air

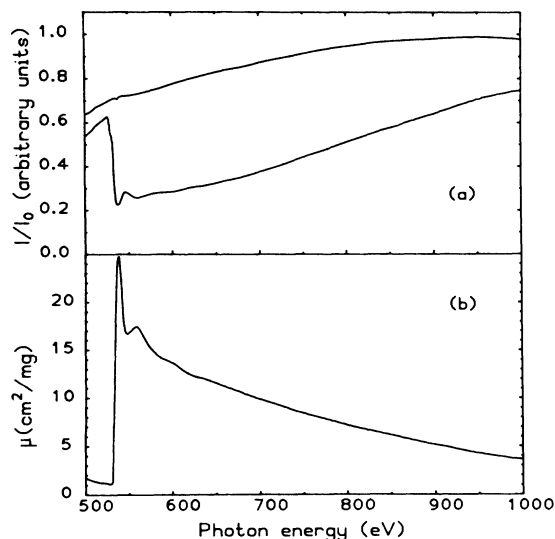


FIG. 2. Absorption spectra of water. (a) Raw data. Top: transmitted flux through an empty cell; bottom: through a water-filled cell. (b) Attenuation coefficient of water.

trapped behind the rear window of the sample cell are also corrected with a spectrum taken with the cell filled with air.

The EXAFS function was extracted by an analysis algorithm specially designed for soft-x-ray spectra.¹¹ The result is shown in Fig. 3, along with two theoretical curves. In calculating these curves we considered only the backscattering from oxygen atoms, used $g_{\text{OO}}(r)$ of heavy water by Kalman, Palinkas, and Kovacs,⁶ and known phase and amplitude functions for the O-O pair: the dot-dashed curve employs the theoretical result by Teo and Lee;¹² the dotted curve employs that derived from a gas-phase O_2 experiment.¹⁰ In both cases the phase and amplitude function are extrapolated down to $k=0 \text{ \AA}^{-1}$. For example, Teo and Lee's results are expressed as

$$\phi_{\text{OO}}(k) = -0.74k - 3.17$$

and

$$F_{\text{O}}(k) = \exp(0.019k^2 - 0.60k + 1.6) .$$

The theoretical curves were normalized to the data. The APCF of heavy water is used because its structural difference from light water is well below the detectable limit of the present experiment.⁵ In treating experimental data, E_0 was chosen at 529 eV , 5 eV below the inflection-point energy in the absorption spectrum, to improve the

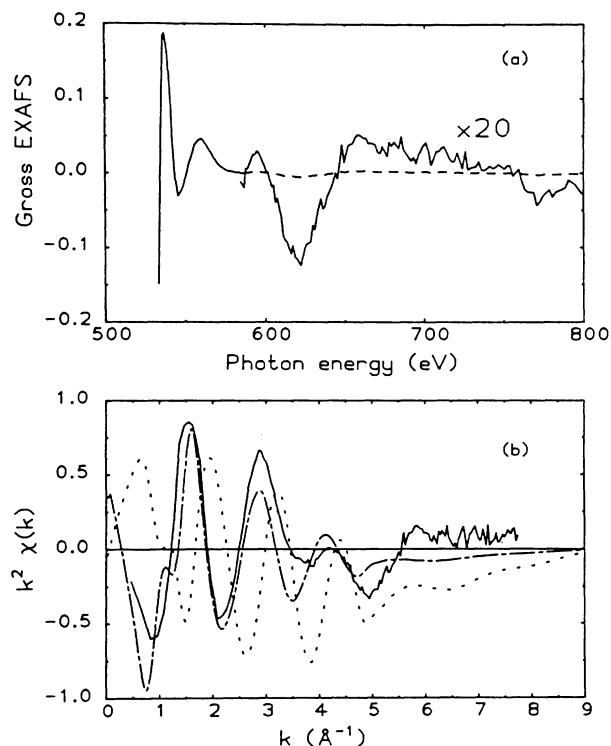


FIG. 3. EXAFS spectra of water. (a) EXAFS spectrum in energy coordinates. (b) EXAFS spectrum in k coordinates. Full curve: experiment; dot-dashed curve: calculation based on Teo and Lee results; dotted curve: calculation based on parameters derived from EXAFS of O_2 .

fit. With these parameters the theoretical curve based on Teo and Lee's (TL) parameters, $\chi_{TL}(k)$, is in qualitative agreement with the experiment. Quadratic and cubic extrapolation of the phase function give similar results. It is interesting that while Teo and Lee's results do not fit small molecules,¹⁰ e.g., O₂, they do work here. This is consistent with the EXAFS studies of amorphous ice.¹³ This may be due to the different length scales involved. In small molecules the interatomic distance is of atomic size (about 2.5 times smaller than in water and ice) and the plane-wave approximation adopted in Teo and Lee's calculation may not be applicable.

There is a significant low-frequency component in the difference $\chi_{\text{expt}}(k) - \chi_{TL}(k)$ (difference in the center lines of the oscillations). We attribute this to the backscattering of the hydrogen atoms in H₂O molecules. We cannot take this into account in our fit for lack of data on the hydrogen backscattering phase and amplitude. Similar low-frequency modulation is also observed in the spectrum of H₂O vapor, but no quantitative conclusions are drawn there due to insufficient signal-to-noise ratio in that experiment.

While the amplitude of the theoretical $k^2\chi(k)$ decreases in a smooth fashion, different behavior is found in the experimental data in the region 3–6 Å⁻¹. The faster decrease of the EXAFS amplitude around 4 Å⁻¹ indicates a broader first-shell peak in $g_{OO}(r)$. The structure near 5 Å⁻¹ is deeper and wider than the theoretical curve. This is indicative of the fact that the first-neighbor peak may have some structure. To illustrate this point, we introduce a function

$$H(k) = k\chi(k)/4\pi\rho_0 F_0(k).$$

For a rough estimate, we neglect the backscattering of hydrogen atoms and the first term (low frequency) in Eq. (1). Using Teo and Lee's phase function, we obtain

$$H(k) \approx - \int_0^\infty (g_{OO} - 1) e^{-2r/\lambda} \times \sin[2k(r - 0.37) - 0.03] dr.$$

The sine transform of $H(k)$ calculated from both χ_{expt} and χ_{TL} , denoted by h_{expt} and h_{TL} , are shown in Fig. 4. h_{TL} roughly reproduces Kalman's $g_{OO}(r)$ but shifted by about 0.37 Å. In h_{expt} the first peak is broader; the first minimum is shifted to larger r and is shallower than h_{TL} . One possible cause of this difference is the focusing effect of the intervening hydrogen atoms. If a hydrogen atom is on the straight line between two oxygen atoms, its atomic potential modifies the backscattering phase and amplitude, and the peak is shifted. The effect may vary significantly as the hydrogen atom moves around its equilibrium position and effectively broadens the observed first-neighbor peak. If this interpretation is correct, the peak width and shape is expected to be sensitive to temperature and zero-point motion of the hydrogen atoms.

Another possible source of the discrepancy concerns the data in the low- k region: Technically $\chi(k)$ is sensitive to the choice of E_0 ; fundamentally the plane-wave single-scattering EXAFS formalism loses its validity, the smoothly extrapolated phase and amplitude lose their physical meaning, and hence the sine transform (Fig. 4)

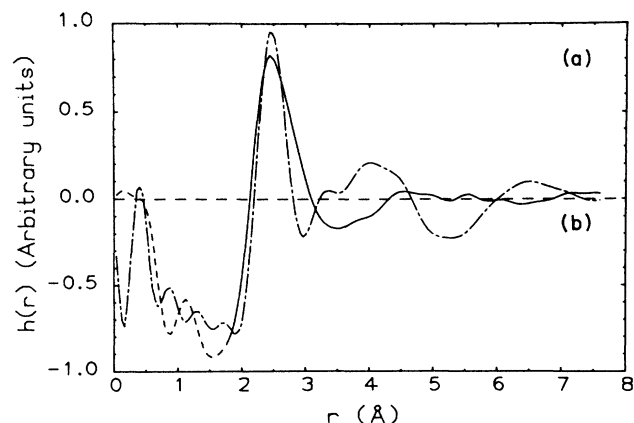


FIG. 4. "Appropriate APCF" derived from EXAFS (see text). Full curve: experiment; dot-dashed curve: theory.

should only be treated as a qualitative guide.

We have also attempted to apply the Fourier transform method commonly used in EXAFS analysis. However, it is not suitable for very disordered systems such as liquids. Figure 5(b) shows the amplitude of the Fourier transform of $\chi(k)$ which has been shifted toward the right by 0.37 Å to compensate for the O-O pair phase shift. The Fourier transform of $\chi(k)$ can be expressed as the convolution

$$f(r) \approx e^{ik+r} \{w(k-r) \otimes [g(r)e^{-r/\lambda} e^{-ik+r}]\},$$

where $k_{\pm} = k_{\text{max}} \pm k_{\text{min}}$ is determined by the available data range ($k_{\text{min}}, k_{\text{max}}$), and $w(k-r)$ is the Fourier transform of the window function used in transforming $\chi(k)$. Since EXAFS data are limited to the positive k region, $k_+ > k_-$, the width of the window is greater than the

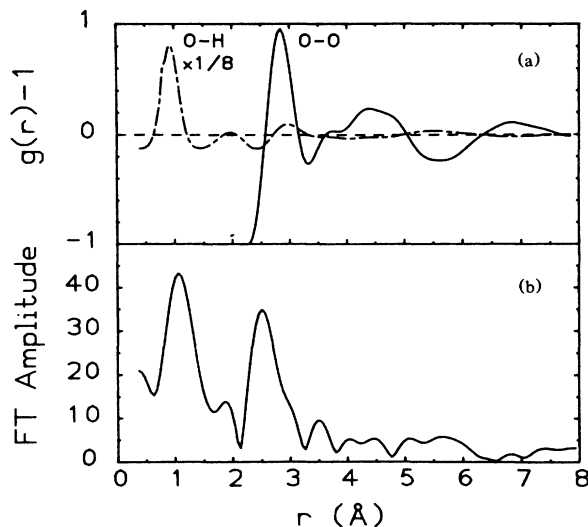


FIG. 5. Fourier transform of $k^2\chi(k)$. (a) APCF's in heavy water (Ref. 6). Full curve: $g_{OO}-1$; dot-dashed curve: $(g_{OH}-1)/8$. (b) The Fourier-transform (FT) amplitude of $k^2\chi(k)$.

period of e^{-ik+r} and $|f(r)|$ is a distorted form of $g(r)$. Only sharp features in $g(r)$ survive the convolution and show up as broadened peaks in $|f(r)|$. In Fig. 5(b) the strong peak at 2.6 Å corresponds to the sharp rise in $g_{OO}(r)$. The peak at 1 Å is likely due to the intramolecular peak in $g_{OH}(r)$. This peak can be affected by the choice of spline fit in the EXAFS analysis program. The spline fit acts like a high-pass filter and its cutoff distorts the experimental EXAFS function and adds spurious features to the Fourier-transformed spectrum in the low- r region, similar to the $g(r)$ derived from diffraction experiments. In diffraction studies, recent comparison between the calculated and observed partial structure function is normally made in k space, since the Fourier transform introduces significant uncertainties.

In summary, the EXAFS of liquid water is observed for the first time. The experimental data are compared with the theory which includes backscattering from oxygen only, with parameters based on Teo and Lee's work. We find qualitative agreement and suggest that the remaining

discrepancy may be attributed partly to hydrogen backscattering, and partly to the focusing effect of the hydrogen atoms between the absorbing and backscattering oxygen atoms. Our limited knowledge about the phase and amplitude function prevents us from a quantitative analysis of the oxygen-hydrogen APCF at this time. The focusing effect, if verified, may open up new possibilities for experiments on liquids and give information on hydrogen bond orientation and its variation with temperature.

We are indebted to Dr. R. Feder for his help with the sample cell design and for the Si_3N_4 windows, and to Professor H. A. Friedman and Dr. E. Behrman for many stimulating and enlightening discussions. This work is supported in part by the Air Force Office of Scientific Research, under Contract No. F-49620-87-K-0001. The National Synchrotron Light Source, where part of this work is performed, is supported by the Department of Energy under Contract No. DE-AC02-76-CH00016.

-
- ¹F. H. Stillinger and A. Rahman, *J. Chem. Phys.* **57**, 1281 (1972); **60**, 1545 (1974); **68**, 666 (1978); O. Matsuoka, E. Clementi, and M. Yoshimine, *ibid.* **64**, 1351 (1976); V. Carravetta and E. Clementi, *ibid.* **81**, 2646 (1984).
- ²R. A. Kuharski and P. J. Rossky, *Chem. Phys. Lett.* **103**, 357 (1984).
- ³A. H. Narten and H. A. Levy, *J. Chem. Phys.* **55**, 2236 (1971); A. H. Narten, Oak Ridge National Laboratory Report No. 4578, 1978 (unpublished).
- ⁴J. E. Enderby and G. W. Neilson, in *Water*, edited by F. Franks (Plenum, New York, 1979).
- ⁵W. E. Thiessen and A. H. Narten, *J. Chem. Phys.* **77**, 2656 (1982).
- ⁶E. Kalman, G. Palinkas, and P. Kovacs, *Mol. Phys.* **34**, 505 (1977); **34**, 525 (1977).
- ⁷T. M. Hayes and J. B. Boyce, *Solid State Phys.* **37**, 173 (1982).
- ⁸G. Bunker and E. A. Stern, *Phys. Rev. Lett.* **52**, 1990 (1984).
- ⁹B. X. Yang, J. Kirz, and I. McNulty, *Proc. SPIE Int. Soc. Opt. Eng.* **689**, 34 (1986).
- ¹⁰B. X. Yang, J. Kirz, and T. K. Sham, *J. Phys. (Paris) Colloq.* **48**, C8-585 (1987).
- ¹¹B. X. Yang and J. Kirz, *Phys. Rev. B* **35**, 6100 (1987).
- ¹²B.-K. Teo and P. A. Lee, *J. Am. Chem. Soc.* **101**, 2815 (1979).
- ¹³R. A. Rosenberg, P. R. LaRoe, V. Rehn, J. Stohr, R. Jaeger, and C. C. Parks, *Phys. Rev. B* **28**, 3026 (1983).